

Angular distribution of evaporated protons from 50-MeV-range proton-nucleus reactions

Yuji Yamaguchi¹, Yusuke Uozumi¹, and Masahiro Nakano²

¹*Kyushu University, Department of Applied Quantum Physics and Nuclear Engineering, 819-0395 Fukuoka, Japan*

²*Junshin Gakuen University, Faculty of Health Sciences, 815-8510 Fukuoka, Japan*

Abstract. The angular distribution of compound reactions at bombarding energies lower than 10 MeV is known to be 90° symmetry. At the higher incident energies, 50-MeV range, the quantization axis tilts from the beam axis due to the particle emission in the cascade or the pre-equilibrium process. Therefore, it is necessary to know the tilted quantization axis for the angular distribution calculation of the evaporated protons from (p, p'x) reactions. In the present work, we applied the intranuclear cascade (INC) model to determine the tilted quantization axis by a classical vector analysis. The proton evaporation was calculated by the generalized evaporation model (GEM). By fitting calculations to experimental angular distributions, we deduced the angular momentum transfer from the equilibrium state.

1 Introduction

The nuclear reactions at bombarding energies higher than 10 MeV/nucleon are interpreted by a two-stage model. The first stage is the cascade or the multi-step direct process, where several energetic particles are emitted during series of intranuclear NN collisions. When the cascade process is finished, the nucleus reaches equilibrium and forms a highly-excited state. The second stage is the particle emission via the decay of the excited nucleus. Since the emitted particles show energy distributions of the Maxwellian shape, it is called the nuclear evaporation process.

Extensive efforts in both theory and experiment were made to understand the nuclear evaporation process for compound reactions at lower energies than 10 MeV/nucleon. A lot of experimental observations show[1] symmetrical angular distributions with respect to 90° in the CM system. This symmetry has been proved theoretically [2] to be ascribable to the angular momentum, which is brought into target nucleus by the incident particle. The angular momentum determines the nuclear level density and the centrifugal barrier, which are essential to interpret the energy distributions of the evaporation process.

In contrast, no theoretical study was made for the evaporation from a highly-excited equilibrium state produced in medium-energy (20-80 MeV) reactions. Since energetic particles are emitted during the first stage, the angular momentum will deviate from the initial value that is brought in by an incident particle. The quantitative analysis of angular momentum is crucial. However, there was no microscopic theory that explains the first stage reasonably with the angular momentum vector, and therefore no quantitative interpretation was performed in the past. The output of previous studies is only some empirical formulations presenting the shapes of angular distributions. Model calculation codes developed recently for general applications ignore the angular momenta and employ an

assumption of the isotropic angular distributions. Indeed, some disagreements have been pointed out between experimental and calculated values. Since we succeeded in development of a reliable model [3,4] for the first stage, the intranuclear cascade (INC) model, it is now possible to estimate the angular momentum vector in a classical way.

The object of the present work is to apply the classical vector analysis to obtain angular momentum of evaporated protons in nuclear reactions induced by protons of medium-energy i.e., around 50-MeV-range protons. The tendency of angular momenta is discussed in terms of the target mass.

2 Model and analysis

2.1 Outline of the first-stage model

The angular momentum vector of cascade residue was calculated by the INC model for the first-stage. The details of the present INC model is given in Refs. [3,4]; here sole the outline is described. The target nucleus is considered to be a sphere containing constituent nucleons with complete isospin degeneracy. Each nucleon has position and momentum and travels inside the nucleus freely. When a nucleon comes close to the other within a distance of the nucleon–nucleon cross section, nucleon–nucleon collision takes place. The inmedium scattering angle is chosen randomly by using experimental angular distributions of nucleon–nucleon cross sections [5]. When all energetic particles are emitted and no nucleons have chance to escape from the target nucleus, the cascade process finishes and the angular momentum vector L_{res} is calculated for residual nucleus in a classical many-body mechanics:

$$L_{res} = L_0 - \sum_{i-emitted} \mathbf{r}_i \times \mathbf{p}_i, \quad (1)$$

where L_0 is the angular momentum brought by an incident particle, and \mathbf{r}_i , \mathbf{p}_i are position and momentum of the emitted particle i , respectively.

2.2 Evaporation model

The Generalized Evaporation Model (GEM) code [6,7] was used to calculate the energy and emission angle of evaporated protons in the present work. It is assumed in GEM that the total emission width Γ_j of a particle j escaping from the parent nucleus i is expressed by

$$\Gamma_j = \frac{(2S_j + 1)m_j}{\pi^2 \hbar^2} \frac{1}{\rho_i(E)} \int_V^{E-Q} \varepsilon \sigma_{inv}(\varepsilon) \rho_d(E - Q - \varepsilon) d\varepsilon, \quad (2)$$

where the symbols ε , m_j , S_j are kinetic energy, mass and spin of the emitted particle j , respectively. Q is the Q -value, V is the Coulomb barrier, and d denotes the daughter nucleus. The inverse reaction cross section σ_{inv} for charged particles is given by

$$\sigma_{inv}(\varepsilon) = \sigma_g \alpha \left(1 - \frac{V}{\varepsilon} \right), \quad (3)$$

where σ_g is the geometric cross section, and α is a parameter. The level density function ρ for the parent and daughter nucleus is calculated based on the Fermi-gas model.

The total emission width of an ejectile j is summed over its ground state and all its excited states. The ejectile j is selected according to the probability distribution p_j calculated by

$$p_j = \frac{\Gamma_j}{\sum_n \Gamma_n}. \quad (4)$$

The original code of GEM employs the assumption that the angular distribution of emitted particles is isotropic in the CM system. In the present work, we modify calculation method for the angular distribution.

2.3 Angular distribution

The angular distribution $W(\theta)$ of evaporated particles from compound system formed by a complete fusion is expressed by

$$W^{com}(\theta) = \sum_{L_{even}} C_L P_L(\cos \theta), \quad (5)$$

where C_L is constants depending on L which is the transferred angular momentum. In the case of emission of particles from a highly-excited nucleus formed in medium-energy reactions, the quantization axis should tilt from the beam axis. Then, we assume the form:

$$W(\theta) = \Lambda_{\theta' \rightarrow \theta} \left| \sum_{L_{even}} C_L P_L(\cos \theta') \right|, \quad (6)$$

where θ' is the emission angle in a new scattering plane defined by the angular momentum vector of residual nucleus, and Λ is a projection operator to the coordinate system of the laboratory frame, where the observation is made (Fig. 1). Since the evaporated protons have low energies, possible transferred angular momenta should be $L = 0$ and 2 in general. We determined the ratio of these transferred angular momenta to fit experimental angular distributions of (p, p'x) reactions at around 50 MeV of incident energies.

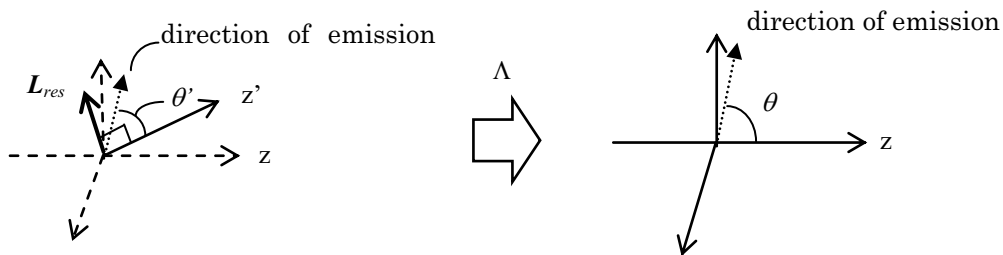


Figure 1. The relation between the emission angle in a new scattering plane and that in the system of the laboratory frame, where the observation is made .

3 Results and discussion

The calculations were carried out for (p, p'x) reactions on target nuclei of ^{27}Al , ^{56}Fe , ^{89}Y , and ^{197}Au at 60-MeV of an incident energy. Angular distributions were made from experimental energy-angle double-differential cross section (DDX) data for emitted protons of energies where evaporation is dominant. The experimental data were taken from EXFOR [8]. Calculated and observed spectral DDXs are shown in Fig. 2 for the 61.5-MeV $^{197}\text{Au}(p, p'x)$ reaction by solid lines and circles, respectively. For the GEM calculation, an assumption of isotropic angular distribution is employed. The evaporation regions are focused and spectra of higher energies than 20 MeV are not displayed in

Fig. 2. The calculated evaporation contribution is also indicated by broken lines. It is found that the energy region of 5 to 7 MeV is governed by the evaporation process.

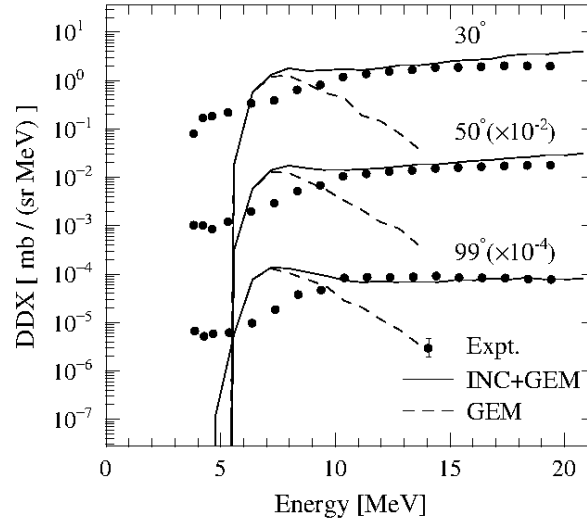


Figure 2. Proton energy spectra from inclusive $^{197}\text{Au}(p, p'x)$ reaction at 61.5 MeV. The angular distribution of GEM calculation is isotropic. The higher-energy parts are not shown, but only the evaporation regions are displayed.

The angle deviation $\Delta\theta$ from the initial quantized axis was calculated by the INC model for the $^{27}\text{Al}(p, p'x)$ and $^{197}\text{Au}(p, p'x)$ reactions at 60-MeV. The resulted $\Delta\theta$ distribution is shown in Fig. 3. The distributions show monotonic decrease for both ^{27}Al and ^{197}Au targets. The average $\Delta\theta$ as a function of incident energy on the ^{197}Au target nucleus is shown in Fig. 4. With increasing incident energy, the average $\Delta\theta$ slightly increases. In Fig. 5, the average $\Delta\theta$ as a function of target mass is shown at 60 MeV. With increasing target mass, $\Delta\theta$ slightly increases and becomes constant for heavier targets.

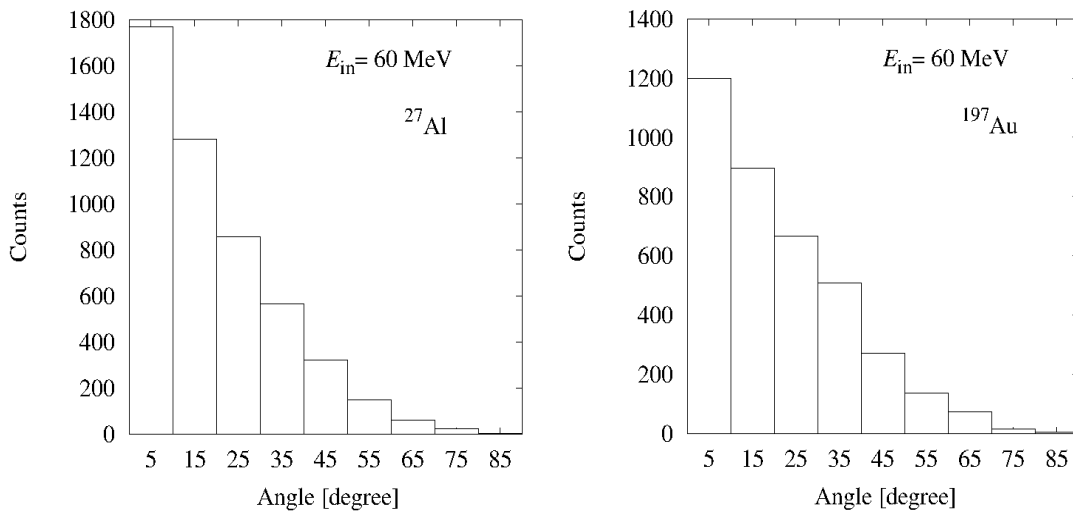


Figure 3. Angle difference of angular momenta from the initial direction for targets of ^{27}Al (left) and ^{197}Au (right).

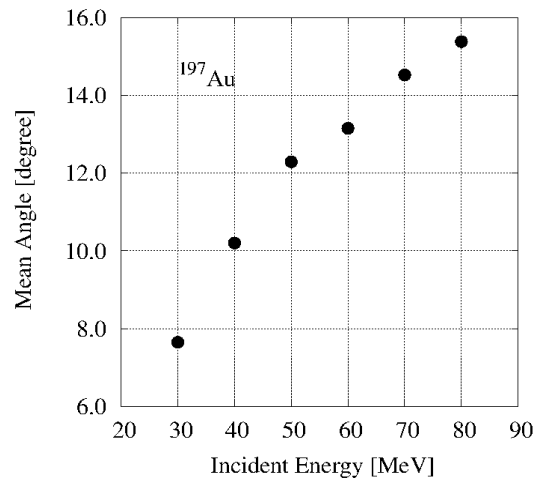


Figure 4. Mean angle difference of angular momenta from the initial direction as function of incident energy.

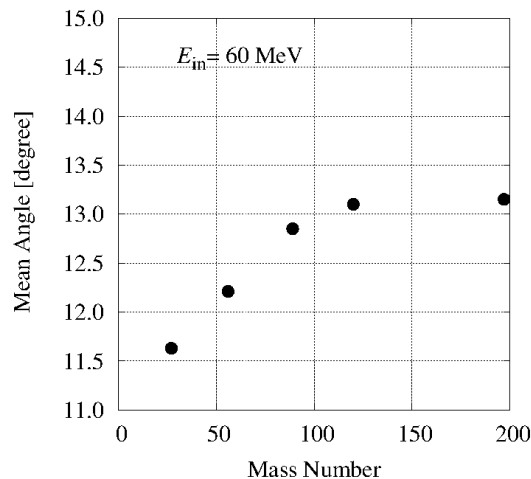


Figure 5. Mean angle difference of angular momenta from the initial direction as function of target mass.

Angular distributions obtained by calculations and experiments are shown in Fig. 6 and Fig. 7 for targets of ^{27}Al , ^{56}Fe in 60-MeV (p, p'x) reactions, respectively. Since transferred angular momentum $L = 0$ is dominant for targets of ^{27}Al and ^{56}Fe , only isotropic results are displayed. The results of $L = 0$ calculations are in good agreements with experiments.

In Fig. 8 and Fig. 9, angular distributions are shown for targets of ^{89}Y and ^{197}Au in 60-MeV (p, p'x) reactions, respectively. Although no experimental data were obtained at backward angles, the experimental data on the ^{197}Au target show much smaller values at 100° than those at forward angles. Thus, the isotropic distribution cannot explain the data of around 90° as illustrated by the dashed curves. In contrast, calculations with $L = 2$ reproduce the observation closely. For the case of the ^{89}Y target, $L = 0$ and 2 ratio of 8:2 was the best to fit the experiments.

From the present results, mass dependence of the ratio of $L = 0$ and 2 was observed. In Fig. 10, target mass dependence of the ratio is shown. For the light targets such as ^{27}Al and ^{56}Fe , angular distributions are explained by $L = 0$ only. With increasing mass, the ratio of $L = 2$ increases. Since the angular momentum L_{res} shows larger values for heavier targets, the angular momentum L of evaporated protons, also, may show larger values.

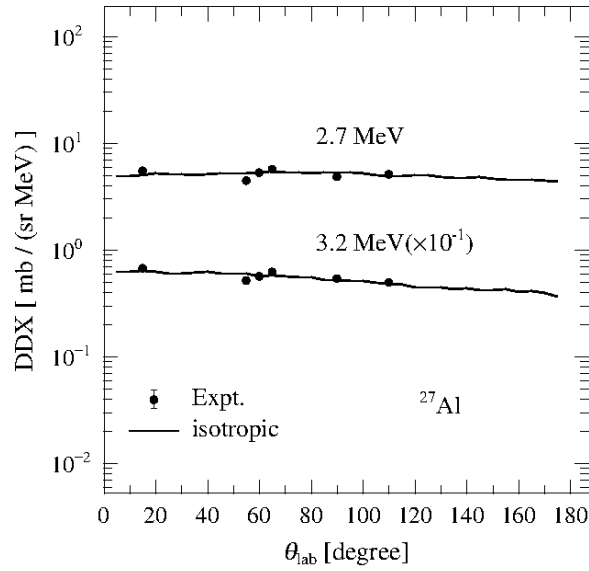


Figure 6. Angular distributions of 2.7- and 3.2-MeV protons from 61.7-MeV $^{27}\text{Al}(p,p'x)$ reactions. Experimental data are shown with closed circles. GEM calculation assuming isotropic angular distribution is shown with the solid line.

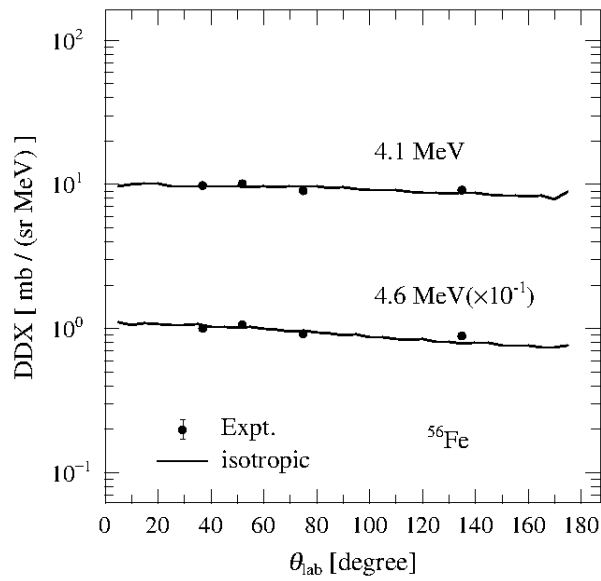


Figure 7. Angular distributions of 4.1- and 4.6-MeV protons from 61.5-MeV $^{56}\text{Fe}(p,p'x)$ reactions. See Fig. 6 caption.

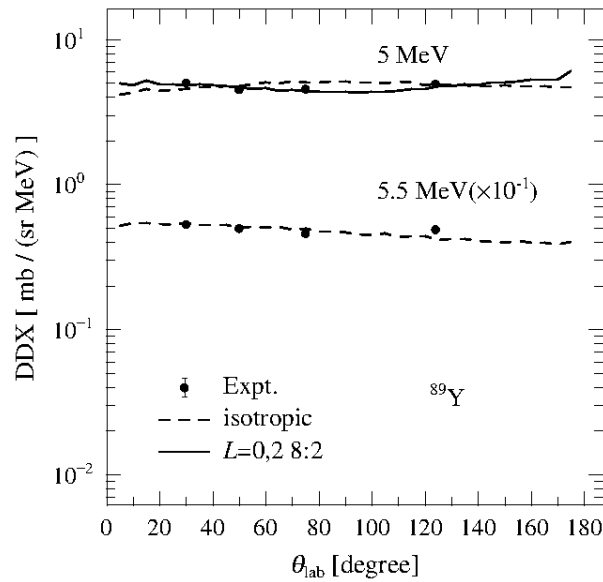


Figure 8. Angular distributions of 5- and 5.5-MeV protons from 61.5-MeV $^{89}\text{Y}(p,p'x)$ reactions. Experimental data are shown with closed circles. GEM calculation assuming isotropic angular distribution is shown with the broken line and present calculation with the solid line.

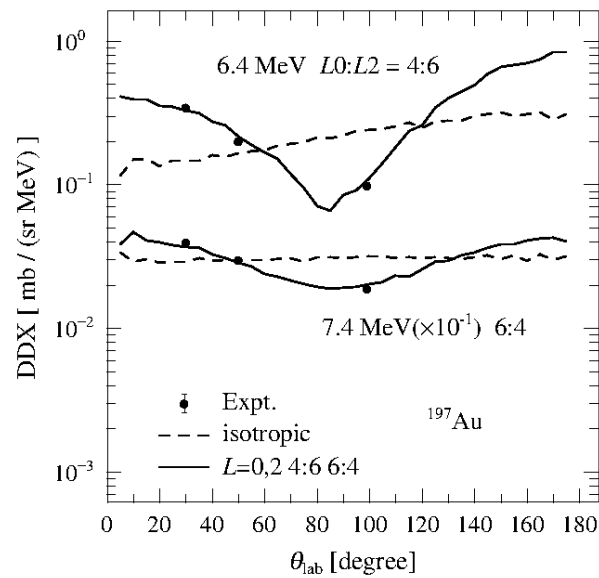


Figure 9. Angular distributions of 6.4- and 7.4-MeV protons from 61.5-MeV $^{197}\text{Au}(p,p'x)$ reactions. See Fig. 8 caption.

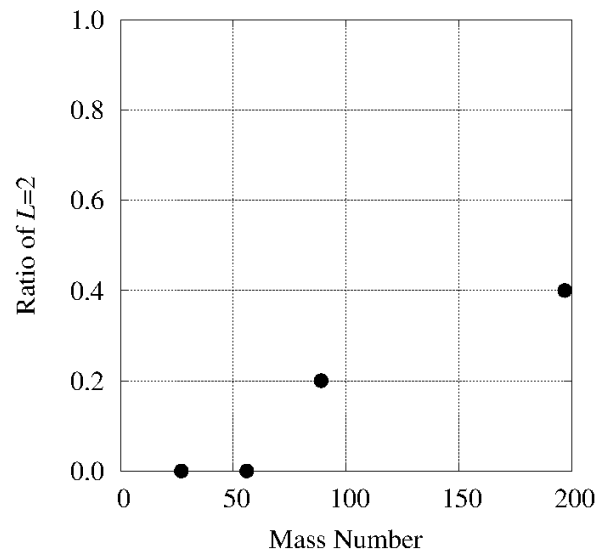


Figure 10. Target mass dependence of the ratio of $L = 2$ to $L = 0$.

4 Conclusion

The classical vector analysis, where the angular momentum is calculated in a classical many-body mechanics in terms of intranuclear cascade model was performed to deduce angular momenta of evaporated protons from medium-energy proton-nucleus reactions. The INC model is applied to extract the angular momentum vector after the cascade process. The mixing ratios of transferred angular momenta in the expression of angular distribution were determined to fit experimental angular distributions. Resultant angular momenta for targets over the periodic table show reasonable mass dependence; angular momenta of evaporated protons show a rising tendency with mass number. Since the angular momentum L_{res} shows larger values for heavier targets, the angular momentum of evaporated protons, also, shows larger values.

References

1. W. J. Knox, A. R. Quinton, C. E. Anderson, Phys. Rev. **120**, 2120–2128, (1960) (therein)
2. T. Ericson, V. Strutinski, Nucl. Phys. **8**, 284–293, (1958)
3. Y. Uozumi, T. Yamada, S. Nogamine, M. Nakano, Phys. Rev. C, **86**, 1–7, (2012)
4. Y. Uozumi, T. Yamada, M. Nakano, Jour. Nucl. Sci. Tech. **52**, 264–273, (2015)
5. J. Cugnon, D. L’Hote, J. Vandermeulen, Nucl. Instr. and Meth. B, **111**, 215–220, (1996)
6. S. Furihata, Adv. Monte Carlo Rad. Trans. Simul and Appl., 1045–1050, (2001)
7. S. Furihata, T. Nakamura, Jour. Nucl. Sci. Tech. **39**, Suppl.2, 758–762, (2002)
8. EXFOR Experimental Nuclear Reaction Data, [https:// www-nds.iaea.org/exfor/exfor.htm](https://www-nds.iaea.org/exfor/exfor.htm).